

University of Groningen

Compressional-mode giant resonances in deformed nuclei

Itoh, M; Sakaguchi, H; Uchida, M; Ishikawa, T; Kawabata, T; Murakami, T; Takeda, H; Taki, T; Terashima, S; Tsukahara, N

Published in:
Physics Letters B

DOI:
[10.1016/S0370-2693\(02\)02892-7](https://doi.org/10.1016/S0370-2693(02)02892-7)

IMPORTANT NOTE: You are advised to consult the publisher's version (publisher's PDF) if you wish to cite from it. Please check the document version below.

Document Version
Publisher's PDF, also known as Version of record

Publication date:
2002

[Link to publication in University of Groningen/UMCG research database](#)

Citation for published version (APA):

Itoh, M., Sakaguchi, H., Uchida, M., Ishikawa, T., Kawabata, T., Murakami, T., Takeda, H., Taki, T., Terashima, S., Tsukahara, N., Yasuda, Y., Yosoi, M., Garg, U., Hedden, M., Kharraja, B., Koss, M., Nayak, B.K., Zhu, S., Fujimura, H., ... Volkerts, M. (2002). Compressional-mode giant resonances in deformed nuclei. *Physics Letters B*, 549(1-2), 58-63. [PII S0370-2693(02)02892-7]. [https://doi.org/10.1016/S0370-2693\(02\)02892-7](https://doi.org/10.1016/S0370-2693(02)02892-7)

Copyright

Other than for strictly personal use, it is not permitted to download or to forward/distribute the text or part of it without the consent of the author(s) and/or copyright holder(s), unless the work is under an open content license (like Creative Commons).

The publication may also be distributed here under the terms of Article 25fa of the Dutch Copyright Act, indicated by the "Taverne" license. More information can be found on the University of Groningen website: <https://www.rug.nl/library/open-access/self-archiving-pure/taverne-amendment>.

Take-down policy

If you believe that this document breaches copyright please contact us providing details, and we will remove access to the work immediately and investigate your claim.

Downloaded from the University of Groningen/UMCG research database (Pure): <http://www.rug.nl/research/portal>. For technical reasons the number of authors shown on this cover page is limited to 10 maximum.



ELSEVIER

Available online at www.sciencedirect.com

SCIENCE @ DIRECT®

PHYSICS LETTERS B

Physics Letters B 549 (2002) 58–63

www.elsevier.com/locate/npe

Compressional-mode giant resonances in deformed nuclei

M. Itoh^a, H. Sakaguchi^a, M. Uchida^a, T. Ishikawa^a, T. Kawabata^a, T. Murakami^a,
H. Takeda^a, T. Taki^a, S. Terashima^a, N. Tsukahara^a, Y. Yasuda^a, M. Yosoi^a, U. Garg^b,
M. Hedden^b, B. Kharraja^b, M. Koss^b, B.K. Nayak^b, S. Zhu^b, H. Fujimura^c,
M. Fujiwara^{c,d}, K. Hara^c, H.P. Yoshida^c, H. Akimune^e, M.N. Harakeh^f, M. Volkerts^f

^a Department of Physics, Kyoto University, Kyoto 606-8502, Japan

^b Physics Department, University of Notre Dame, Notre Dame, IN 46556, USA

^c Research Center for Nuclear Physics (RCNP), Osaka University, Osaka 560-0047, Japan

^d Advanced Science Research Center, Japan Atomic Energy Research Institute, Tokai, Ibaraki 319-1195, Japan

^e Department of Physics, Konan University, Hyogo 658-8501, Japan

^f Kernfysisch Versneller Instituut (KVI), NL 9747 AA Groningen, The Netherlands

Received 16 July 2002; received in revised form 4 September 2002; accepted 18 October 2002

Editor: V. Metag

Abstract

Background-free inelastic scattering spectra have been obtained for the Sm isotopes with 400 MeV α particles at forward angles (including 0°) to investigate the effect of deformation on the compressional-mode giant resonances. The strength distributions for the isoscalar giant resonances ($L \leq 3$) have been extracted for the spherical nucleus ^{144}Sm and the deformed nucleus ^{154}Sm . We have observed that the effects of deformation are different for the low- and high-excitation-energy components of the isoscalar giant dipole resonance in ^{154}Sm . Evidence for the theoretically predicted coupling between the isoscalar dipole resonance and the high-energy octupole resonance is reported.

© 2002 Elsevier Science B.V. Open access under [CC BY license](#).

PACS: 24.30.Cz; 25.55.Ci; 27.60.+j; 27.70.+g

The giant monopole resonance (GMR) and the isoscalar giant dipole resonance (ISGDR) are of considerable interest since their excitation energies directly relate to the incompressibility of nuclear matter, an important component of the nuclear equation of state which plays a crucial role in describing nucleon motion in nuclei, and is also related to the type II supernova explosions.

It was reported about two decades ago that the giant resonance “bump” in the deformed nucleus had a larger “lower” component when compared with that in the spherical nuclei. This was interpreted as implying that the GMR splits into two components because of coupling with the $K = 0$ component of the giant quadrupole resonance (GQR) [1,2]. However, because of large instrumental backgrounds, it was difficult to reach a definitive conclusion. Recently, Youngblood et al. [3] extracted the E0 and E2 strength distributions in ^{154}Sm , and reported evidence for the

E-mail address: itoh@rcnp.osaka-u.ac.jp (M. Itoh).

coupling between the GMR and GQR by fitting the observed $L = 0$ and $L = 2$ strength distributions with the predicted number of Gaussian peaks from the adiabatic cranking model [4]. Their results showed a fair agreement with the calculations of Abgrall et al. [4] but not with several other calculations [5–8].

Although the effects of coupling between the GMR and GQR in deformed nuclei, resulting in splitting of the GMR and broadening of the GQR, have been observed in previous measurements, there have been no published data so far on the ISGDR and the high energy octupole resonance (HEOR) in deformed nuclei. On the theoretical side, Nishizaki and Andō had predicted the K -splitting and the coupling between the ISGDR and HEOR some time ago [9]. In this Letter, we report the results on both compressional-modes, the GMR and ISGDR, for the spherical nucleus ^{144}Sm and for the deformed nucleus ^{154}Sm . In particular, the effect of deformation on the ISGDR has been investigated for the first time and evidence has been obtained for the theoretically-predicted coupling between the ISGDR and HEOR.

The experiments were performed at the Research Center for Nuclear Physics (RCNP), Osaka University. $^4\text{He}^{++}$ beams were accelerated by the AVF cyclotron and the ring cyclotron up to 400 MeV. The halo-free beam bombarded thin (2–10 mg/cm²), self-supporting, metallic targets of ^{144}Sm , ^{148}Sm , ^{150}Sm , ^{152}Sm and ^{154}Sm . Here, results are presented only on the ^{144}Sm (spherical) and ^{154}Sm (deformed) nuclei in order to focus the discussion on the effects of deformation.

Inelastically-scattered particles were analyzed by a magnetic spectrometer, Grand Raiden [10]. The vertical and horizontal positions in the focal plane were determined by a focal-plane detector system consisting of two multi-wire drift chambers (MWDCs) and two plastic scintillation counters. The angular distributions were measured with three different settings of the spectrometer system; details of the experimental settings are provided in Refs. [11,12]. The typical energy resolution was ~ 200 keV, sufficient to investigate the giant resonances of interest, with a width of ~ 5 MeV.

In Grand Raiden, particles scattered from the target are focused vertically and horizontally at the focal plane. On the other hand, instrumental background events due to rescattering of α particles on the wall

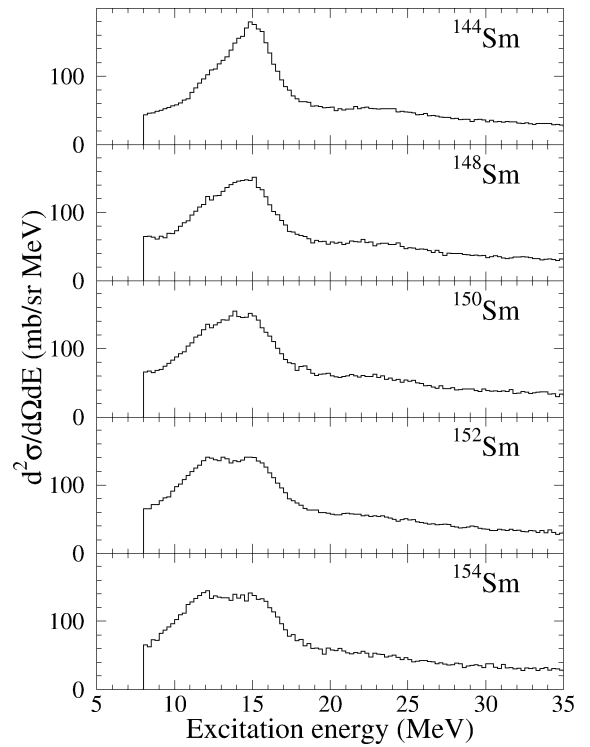


Fig. 1. Inelastic α scattering spectra $E_\alpha = 400$ MeV at 0° ($\theta_{\text{average}} = 0.7^\circ$) for $^{144-154}\text{Sm}$.

and pole surfaces of the spectrometer are not focused in the vertical direction. We obtained clean spectra by subtracting events at the off-median plane from those at the median plane [12]. Energy spectra were obtained in the energy range of $8 < E_x < 33$ MeV over several angles between 0° and 9° (13.5° for ^{144}Sm). The energy spectra at 0° (average angle 0.7°) are shown in Fig. 1 for the Sm isotopes.

In order to identify strengths corresponding to different giant resonances, we have carried out a multipole-decomposition (MD) analysis [13] of the differential cross sections for each 1 MeV bin. In this method, the cross sections $(\frac{d^2\sigma}{d\Omega dE})^{\text{exp}}$ are expressed as the sum of the contributions from the various multipole components:

$$\left(\frac{d^2\sigma}{d\Omega dE}\right)^{\text{exp}} = \sum_L a_L(E_x) \left(\frac{d^2\sigma}{d\Omega dE}\right)_L^{\text{calc}},$$

where E_x is the excitation energy and $(\frac{d^2\sigma}{d\Omega dE})_L^{\text{calc}}$ are the distorted wave Born approximation (DWBA) cross

sections exhausting the full energy-weighted sum rule (EWSR) for the transferred angular momentum L . The fractions of the EWSR, $a_L(E_x)$, for various multipole components were determined by minimizing χ^2 . The physical continuum is included in the MD analysis, since the (α, α') spectra obtained in our measurements are free from any “non-physical” background.

In the DWBA calculations with the code ECIS95 [14], a folded-potential model was employed, with a nucleon- α interaction of the density-dependent Gaussian form, as described in Refs. [15,16]. The nucleon- α interaction is given by:

$$V(|r - r'|, \rho_0(r')) \\ = -(V + iW)(1 - \alpha\rho_0(r')^{2/3}) \exp(-|r - r'|^2/\beta),$$

where the ground-state density $\rho_0(r')$ is unfolded by using the charge density distributions of the Fourier-Bessel expansion form taken from Ref. [17]. To obtain the interaction parameters, we measured elastic scattering of α particles from ^{144}Sm at $E_\alpha = 400$ MeV and fitted the angular distributions with a single-folded potential; the interaction parameters were extracted to be $V = 25.1$ MeV, $W = 14.2$ MeV, $\alpha = 1.9$ fm² and $\beta = 4.5$ fm².

To simplify the calculations, macroscopic transition densities were used. These transition densities are described by Satchler [18] for the GMR ($L = 0$), the isovector giant dipole resonance (IVGDR) ($L = 1$, $T = 1$) and $L \geq 2$ (BM transition density in Ref. [18]), and for the ISGDR by Harakeh and Dieperink [19]. Multipole components up to $L = 14$ for ^{144}Sm , and $L = 10$ for ^{154}Sm were taken into account in the fit, because the first maximum of the angular distribution for the $L = 14$ transfer appears at 13° and for the $L = 10$ at 9° . Use of $L \geq 14$ multipoles in the fits resulted in negligible change in the extracted distributions for $L = 0, 1, 2, 3$. The strength distributions of the IVGDR were fixed by using those deduced from the photo-neutron cross sections [20]. Since the experimental cross sections were obtained from the summation of the yield of the scattering particles within the acceptance of Grand Raiden, the calculated cross sections, $(\frac{d\sigma^2}{d\Omega dE})_L^{\text{calc}}$, were also folded over that angle. Fig. 2 shows the results of typical multipole fits to angular distributions for ^{144}Sm and ^{154}Sm .

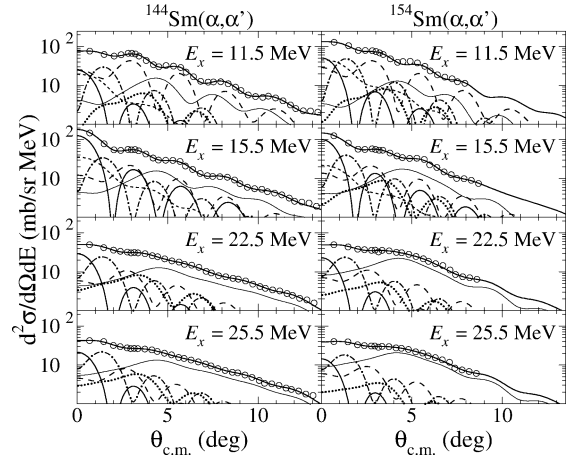


Fig. 2. Double-differential cross sections for selected energy bins in ^{144}Sm and ^{154}Sm . The fits to the data from multipole decomposition are shown. In each panel, the contributions from $L = 0$ (thick solid), $L = 1$ ($T = 0$) (dot-dashed), $L = 1$ ($T = 1$) (dashed), $L = 2$ (long-dashed), $L = 3$ (dotted), and $L \geq 4$ (thin solid) are also displayed.

The strength distributions are expressed as:

$$S_0(E_x) = \frac{2\pi\hbar^2 A \langle r^2 \rangle}{m E_x} a_0(E_x),$$

$$S_1(E_x) = \frac{\hbar^2 A}{32\pi m E_x} \left(11 \langle r^4 \rangle - \frac{25}{3} \langle r^2 \rangle^2 - 10 \epsilon \langle r^2 \rangle \right) \\ \times a_1(E_x),$$

$$S_{L \geq 2}(E_x) = \frac{\hbar^2 A}{8\pi m E_x} L(2L+1)^2 \langle r^{2L-2} \rangle a_L(E_x),$$

where m , A , $\langle r^N \rangle$, ϵ , and $a_L(E_x)$ are the nucleon mass, the mass number, the N th moment of the ground-state density, $\epsilon = (4/E_2 + 5/E_0)\hbar^2/3mA$ (E_0 , E_2 are the centroid energies of the GMR and the GQR, respectively), and the respective EWSR fractions obtained by our MD analysis.

The results for the $L = 0$ and $L = 2$ strength distributions are shown in Fig. 3. Both the GMR and GQR strengths have a well-defined peak but extend to high excitation energies. The EWSR fractions integrated over measured excitation energies are about 200%. The cross section for each L component is well separated by a MD analysis. However, the strength distributions obtained from the comparison with the DWBA cross sections depend on the transition densities used in the analysis. Thus, a possible reason of these ex-

cesses in the EWSR fractions is that the macroscopic transition densities of the GMR and the GQR used in this analysis are not valid in the high excitation energy region. Therefore, further analysis was carried out for the energy region, 8 to 19 MeV for the GMR and 9 to 15 MeV for the GQR. In ^{144}Sm , the GMR and the GQR were each fitted with a Breit–Wigner function. The fitting parameters are listed in Table 1, to-

gether with the EWSR fractions obtained by integrating $E_x S_L(E_x)$ from 8 to 33 MeV. If the shape of the high excitation energy tail is assumed to be a polynomial function, the centroid energies are not affected, but the widths and the EWSR fractions are affected by 20–30%.

The GMR strength is expected to split into two components because of the coupling to the GQR. For comparison with the theoretical results, the “peak region” of the GMR in ^{154}Sm was fitted with two Breit–Wigner functions. The widths were fixed by using those of the GMR and GQR in ^{144}Sm .

The GQR strength, on the other hand, is predicted to split into three components by Abgrall et al. [4] and four components by Nishizaki and Andō [9]. However, the strength distributions for the GQR were well fitted with only two Breit–Wigner functions in the excitation energy region from 9 to 15 MeV. This two-component fit is consistent with very small strengths associated with other components in the theoretical predictions. The results of the fits for ^{154}Sm are also presented in Table 1, previous results from Refs. [3,21] and [22] are also included for comparison.

Fig. 4 compares the centroid energies of each component with those from the two theoretical models viz. the adiabatic cranking model [4] and the fluid-dynamical model [9]. Both the models reproduce the peak energy of the high-excitation-energy (HE) component of the GMR. However, the low-excitation-energy (LE) component is higher in energy than the

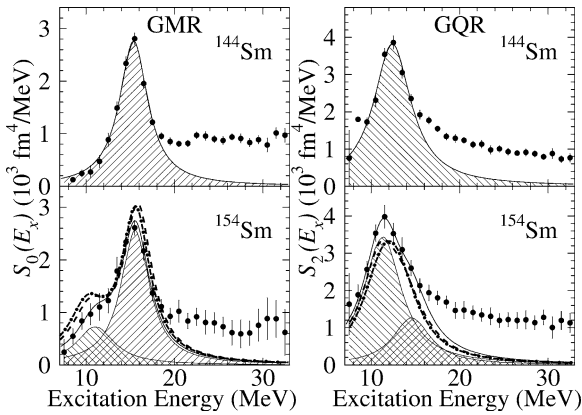


Fig. 3. The $L = 0$ and $L = 2$ strength distributions for $^{144,154}\text{Sm}$ obtained from the multipole-decomposition analysis. The solid lines show the fits with two Breit–Wigner functions to the peak regions. The low- and high-excitation-energy components of the GMR and the GQR are indicated by hatched areas. In ^{154}Sm , the strength distribution obtained in the adiabatic cranking model (dashed lines) [4] and the fluid-dynamical model (dash-dotted lines) [9] are also drawn. Both the calculated strengths are assumed to exhaust the predicted EWSR fractions from 8 to 33 MeV.

Table 1

The parameters for fits to the strength distributions of the GMR and GQR compared with the results in Refs. [3,21,22]. The centroid energy E_0 , width Γ , the EWSR fractions obtained in the Breit–Wigner fits (F) are listed

	Target	LE component			HE component		
		E_0 (MeV)	Γ (MeV)	F (%EWSR)	E_0 (MeV)	Γ (MeV)	F (%EWSR)
GMR	^{144}Sm	–	–	–	15.4 ± 0.1	3.9 ± 0.2	84 ± 5
		–	–	–	15.39 ± 0.28^c	–	–
	^{154}Sm	11.0 ± 0.8 12.1 ± 0.4^c	$(5.1)^a$ –	17 ± 5 36 ± 10^c	15.6 ± 0.2 15.5 ± 0.3^c	$(3.9)^b$ –	69 ± 5 68 ± 9^c
GQR	^{144}Sm	12.4 ± 0.1 12.2 ± 0.2^c	5.1 ± 0.3 2.4 ± 0.2^c	120 ± 10 45 ± 15^c	– –	– –	– –
	^{154}Sm	11.3 ± 0.3 11.3 ± 0.2^c	$(5.1)^a$ –	84 ± 18 44 ± 7^c	14.6 ± 1.9 14.5 ± 0.5^c	$(5.1)^a$ –	41 ± 16 44 ± 8^c

^a The width of the GQR in ^{144}Sm .

^b The width of the GMR in ^{144}Sm .

^c Taken from Refs. [3,21,22].

theoretically predicted values. A similar behavior has been observed for ^{154}Sm by Youngblood et al. [3].

Fig. 3 also shows a comparison between the fits with two Breit–Wigner functions to the GMR and GQR peaks in ^{154}Sm and the strength distributions obtained in the two theoretical models. The theoretical GMR strength was folded with two Breit–Wigner functions. The width of the LE component coupling to the $K = 0$ component of the GQR was taken to be equal to that of the GQR, and the width of the HE component as equal to that of the GMR in ^{144}Sm . For the GQR strength distributions, three or four Breit–Wigner functions were employed, each with a width equal to that of the GQR and the width of the coupling state to the GMR as equal to that of the GMR in ^{144}Sm . In addition, the strength distributions were shifted to a higher excitation energy by 0.6 MeV. As shown in Fig. 3, the experimental GMR and GQR strength distributions are in excellent agreement with both the theoretical models, except the slight shift in the GQR energy.

The isoscalar odd-parity giant resonances, ISGDR and HEOR, are also expected to couple, resulting in shifting of the strengths to lower excitation energies and broadening of the width of HEOR and ISGDR because of the K -splitting [9]. The results of the MD analysis for the ISGDR and the HEOR are shown in Fig. 5. The EWSR fractions are 120–130% in the ISGDR, and 50–60% in the HEOR. In the spherical nucleus ^{144}Sm , the ISGDR strength has two distinct components as reported in Refs. [23,24], and the HEOR strength has a bump peaking at $E_x \sim 22$ MeV. In the deformed nucleus ^{154}Sm , on the other hand, the LE component of the ISGDR strength appears to split into two components ($K = 0$ and $K = 1$) and to be enhanced, whereas the HE component does not show any significant change. For the HEOR, the strength distribution is rather broad, without a discernible peak, and the strength is shifted toward low excitation energies. This broadening of the HEOR in deformed nuclei and the strength shift to lower excitation energies were reported also by Morsch et al. [25].

Although the ISGDR and HEOR strengths for ^{154}Sm would normally be expected to be $\sim 30\%$ higher than those for ^{144}Sm due to the differences in the nuclear masses and radii. These would be further enhanced in ^{154}Sm because of the deformation-induced coupling between the ISGDR and HEOR

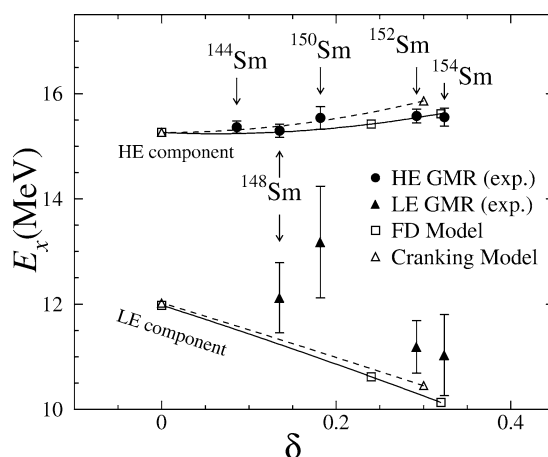


Fig. 4. The peak energies for the HE (closed circles) and LE components (closed triangles) of the GMR are plotted as a function of the deformation parameter δ . The open squares are the peak energies for the GMR predicted the fluid-dynamical (FD) model [9], and the open triangles are those of the cranking model [4]. The lines are drawn to guide the eye.

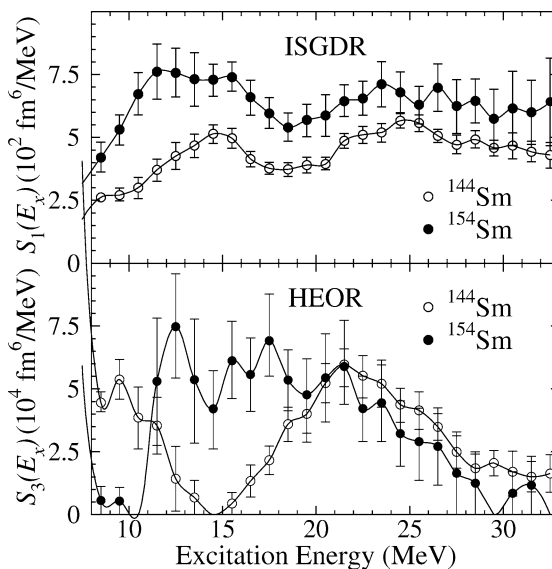


Fig. 5. Comparison of the ISGDR and HEOR strength distributions in ^{144}Sm and ^{154}Sm . The solid lines are drawn to guide the eye. The HEOR strength in ^{154}Sm is enhanced at $E_x = 12.5 \sim 17$ MeV where the LE component of the ISGDR exists.

for the $K = 0$ and $K = 1$ components. In fact, the enhancement of both the ISGDR and HEOR strengths near $E_x \sim 12.5$ MeV in ^{154}Sm , in comparison with ^{144}Sm , is 50–100%, which is significantly larger

than expected simply from mass and radius effects mentioned above. This is inferred to be evidence for a coupling between the two modes. A direct comparison of the observed ISGDR strength in ^{154}Sm with theoretical predictions is, however, complicated by the nature of the LE component of the ISGDR in spherical nuclei. According to recent theoretical work on the ISGDR [26–30], this LE component is of “non-bulk” origin—only the HE component of the ISGDR strength corresponds to a compressional-mode. On the other hand, considering the effects of deformation on the ISGDR and HEOR, Ref. [9] takes into account only the coupling between the HEOR and the compressional-mode ISGDR. Further theoretical work to investigate the effect of deformation on the “non-bulk” LE component of the ISGDR strength is clearly most urgently warranted.

In summary, clean inelastic scattering spectra, free from instrumental background, have been measured for the $^{144}\text{--}^{154}\text{Sm}$ nuclei. The spectra have been decomposed into contributions of various multipoles by a multipole decomposition analysis using DWBA angular distributions obtained in the framework of the density-dependent single-folding model. The strength distributions for the GMR, ISGDR, GQR and HEOR have been determined for the spherical nucleus ^{144}Sm and the deformed nucleus ^{154}Sm . A coupling between the GMR and GQR, and the broadening of the GQR width have been confirmed in the deformed nucleus ^{154}Sm . The strength distributions of the GMR and GQR in ^{154}Sm are in good agreement with the calculations by Abgrall et al. [4] and by Nishizaki and Andō [9]. For the ISGDR, the effects of deformation are different for the low- and high-excitation-energy components in ^{154}Sm . The coupling between the ISGDR and HEOR has been evidenced by enhancement and splitting of the low-excitation-energy component of the ISGDR, the broadening of the HEOR, and the shift of the HEOR strength towards lower excitation energies.

Acknowledgements

We gratefully acknowledge the RCNP cyclotron staff for providing halo-free beams. This work was

supported in part by the US–Japan Cooperative Science Program of the JSPS and the US National Science Foundation (grants Nos. INT-9910015 and PHY-9901133), and the University of Notre Dame.

References

- [1] M. Buenerd, et al., Phys. Rev. Lett. 45 (1980) 1667.
- [2] U. Garg, et al., Phys. Rev. Lett. 45 (1980) 1670.
- [3] D.H. Youngblood, Y.-W. Lui, H.L. Clark, Phys. Rev. C 60 (1999) 067302.
- [4] Y. Abgrall, et al., Nucl. Phys. A 346 (1980) 431.
- [5] T. Kishimoto, et al., Phys. Rev. Lett. 35 (1975) 552.
- [6] T. Suzuki, D.J. Rowe, Nucl. Phys. A 289 (1977) 461.
- [7] N. Auerbach, A. Yeverechyahu, Phys. Lett. 62B (1976) 143.
- [8] D. Zawischa, J. Speth, D. Pal, Nucl. Phys. A 311 (1978) 445.
- [9] S. Nishizaki, K. Andō, Prog. Theor. Phys. 73 (1985) 889.
- [10] M. Fujiwara, et al., Nucl. Instrum. Methods Phys. Res. A 422 (1999) 484.
- [11] M. Itoh, et al., RCNP Annu. Rep. (1999) 7.
- [12] M. Itoh, et al., Nucl. Phys. A 687 (2001) 52c.
- [13] B. Bonin, et al., Nucl. Phys. A 430 (1984) 349.
- [14] J. Raynal, Computer code, ECIS95, NEA0850-14.
- [15] G.R. Satchler, D.T. Khoa, Phys. Rev. C 55 (1997) 285.
- [16] A. Kolomiets, O. Pochivalov, S. Shlomo, Phys. Rev. C 61 (2000) 034312.
- [17] H. De Vries, et al., At. Data Nucl. Data Tables 36 (1987) 495.
- [18] G.R. Satchler, Nucl. Phys. A 472 (1987) 215.
- [19] M.N. Harakeh, A.E.L. Dieperink, Phys. Rev. C 23 (1981) 2329.
- [20] S.S. Dietrich, B.L. Berman, At. Data Nucl. Data Tables 38 (1988) 199.
- [21] D.H. Youngblood, H.L. Clark, Y.-W. Lui, Phys. Rev. Lett. 82 (1999) 691.
- [22] D.H. Youngblood, et al., Phys. Rev. C 23 (1981) 1997.
- [23] H.L. Clark, Y.-W. Lui, D.H. Youngblood, Phys. Rev. C 63 (2001) 031301(R).
- [24] M. Uchida, et al., in preparation.
- [25] H.P. Morsch, et al., Phys. Lett. B 119 (1982) 311.
- [26] I. Hamamoto, H. Sagawa, X.Z. Zhang, Phys. Rev. C 57 (1998) R1064.
- [27] G. Colo, et al., Phys. Lett. B 485 (2000) 362.
- [28] J. Pikarewicz, Phys. Rev. C 62 (2000) 051304(R).
- [29] D. Vretenar, A. Wandelt, P. Ring, Phys. Lett. B 487 (2000) 334.
- [30] S. Shlomo, A.I. Sanzhur, Phys. Rev. C 65 (2002) 047308.